

Measurement of the spectrally-resolved absolute phase difference between orthogonal optical modes using a nonlinear beat signal

Anastassia Gosteva, Markus Haiml, and Ursula Keller

ETH Zurich, Physics Department, Institute of Quantum Electronics,
Wolfgang-Pauli-Str. 16, 8093 Zürich, Switzerland
gosteva@phys.ethz.ch

Abstract: On the basis of white-light interferometry with spectrally integrated detection and Fourier transform (FT) analysis, we demonstrate a novel technique for measuring the spectrally-resolved absolute phase difference between orthogonal optical modes with milliradian precision. The phase difference is evaluated from a nonlinear beat signal, occurring in the phase spectrum when independent interferograms, formed by individual modes, are recorded simultaneously. Although scanning white-light FT interferometry is a linear technique in general, the nonlinear beat signal is due to spectral amplitude variations in each mode. These proof-of-principle absolute phase difference measurements were carried out with polarization and spatial fiber modes.

©2005 Optical Society of America

OCIS codes: (120.3180) Interferometry; (120.5050) Phase measurement; (070.2590) Fourier transform.

References and links

1. M. Born and E. Wolf, *Principles of Optics*. (U. K.: Pergamon, London, 1984).
2. R.M.A. Azzam and N.M. Bashara, *Ellipsometry and Polarized Light*. (North-Holland, Amsterdam, 1987).
3. K. Naganuma, K. Mogi, and H. Yamada, "Group-delay measurement using the Fourier transform of an interferometric cross correlation generated by white light," *Opt. Lett.* **15**, 393-395 (1990).
4. M. Beck and I. A. Walmsley, "Measuring of group delay with high temporal and spectral resolution," *Opt. Lett.* **15**, 492-496 (1990).
5. A. P. Kovacs, K. Osvay, Zs. Bor, and R. Szipocs, "Group-delay measurement on laser mirrors by spectrally resolved white-light interferometry," *Opt. Lett.* **20**, 788-790 (1995).
6. C. Iaconis and I. A. Walmsley, "Spectral Phase Interferometry for Direct Electric Field Reconstruction of Ultrashort Optical Pulses," *Opt. Lett.* **23**, 792-794 (1998).
7. I. A. Walmsley, L. Waxer, and C. Dorrer, "The role of dispersion in optics," *Rev. Sci. Instrum.* **72**, 1-29 (2001).
8. A. Gosteva, M. Haiml, R. Paschotta, and U. Keller, "Noise-related resolution limit of dispersion measurements with white-light interferometers," *J. Opt. Soc. Am B* **22**, 1868-1874 (2005).
9. P. Pavlicek and G. Hausler, "White-light interferometer with dispersion: an accurate fiber-optic sensor for the measurement of distance," *Appl. Opt.* **44**, 2978-2983 (2005).
10. K. Oka and T. Kato, "Spectroscopic polarimetry with a channeled spectrum," *Opt. Lett.* **24**, 1475-1477 (1999).
11. G. Nomarski, "A double-shear differential interferometer using birefringent beamsplitter," *Jap. J. Appl. Phys.* **14**, 363-368 (1975).
12. H. K. Heinrich, D. M. Bloom, and B. R. Hemenway, "Noninvasive sheet charge density probe for integrated silicon devices," *Appl. Phys. Lett.* **48**, 1066-1068 (1986).
13. U. Keller, S. K. Diamond, B. A. Auld, and D. M. Bloom, "A noninvasive optical probe of free charge and applied voltage in GaAs devices," *Appl. Phys. Lett.* **53**, 388-390 (1988).
14. Mitsuo Takeda, Hideki Ina, and Seiji Kobayashi, "Fourier-transform method of fringe-pattern analysis for computer-based topography and interferometry," *J. Opt. Soc. Am. B* **72**, 156-160 (1982).

1. Introduction

Optical modes with different polarization or spatial profiles may experience different phase retardations propagating in optical media or being reflected from optical interfaces [1], [2]. The standard method to measure the phase retardation accumulated in a device under test (DUT) is based on interferometry [3]-[8]. However, the exact determination of phase retardations requires in most cases a meticulous calibration of the zero path length difference between the interferometer arms [9]. Therefore in most interferometric schemes, including scanning white light interferometry [3], the phase is determined within an additive ambiguity. Only the second derivative of the optical phase with respect to angular frequency (i.e. group delay dispersion, GDD) is obtained with precisely [8] known accuracy.

In the present paper we demonstrate a new interferometric technique for measuring the absolute phase difference between collinear orthogonal optical modes, occurring inside the DUT. There are several techniques relying on such phase differences between polarization modes. For instance, the state of polarization of light can be determined from the measurement of the spectrally resolved Stokes parameters [10]. The differential interference contrast of the Nomarski microscope [11] produces an enhanced image contrast with a pseudo relief effect. A similar scheme is applied for noninvasive optical sampling of electrical circuits [12], [13]. Another non-destructive optical technique, ellipsometry [2], analyses the state of polarization of the light that is reflected from the DUT. In these methods an interference pattern is created by means of a polarizer, which projects both polarization modes on a common axis. However, there is no easy way to select a single spatial mode from a collinear beam of spatial modes, or to create interference between them. In contrast, our method is based on a nonlinear beat signal in the phase spectrum when the white-light interferograms of non-interfering orthogonal optical modes in a DUT are recorded simultaneously. As we explain later in the paper, the origin of this nonlinear beat signal is not the interference between the modes itself, but the amplitude-to-phase coupling in the evaluation algorithm.

To illustrate the potential of the method, we measured the spectrally resolved absolute phase difference between two polarization modes and two spatial fiber modes. Moreover, the qualitative and quantitative analysis of the measured data emphasizes a possible and significant source of errors in dispersion measurements with white light interferometers.

2. Method

Lets consider a situation when a single optical mode propagates through a scanning Michelson interferometer with nearly equal arm length, as shown in Fig. 1. By scanning one of the arms, and recording an interference pattern at the output end of the interferometer with a spectrally integrating detector (photodiode), one can access the complex reflectivity or transmission of the DUT simultaneously for all spectral components of the light source.

The GDD is calculated from the Fourier Transform (FT) of the recorded interferogram into the spectral domain. Only the imaginary part is then used to determine the second derivative of the optical phase with respect to the angular frequency (i.e. the GDD). The arm displacement is obtained with sub-nm precision from an interference trace of a separate reference beam by means of a phase retrieval algorithm [14]. This is the standard technique for measuring the dispersion of various optical components over a broadband spectral range, referred to as spectrally integrated white light interferometry [3].

However, if more than one optical mode enters the interferometer, the recorded Fourier phase can be somewhat different than the average phase retardation occurring in each mode during the propagation inside the interferometer. For example, when two optical modes enter the interferometer and each of them experience a slightly different phase variation during propagation (e.g., through a birefringent element or dielectric multilayer structure, or even reflection under non-normal incidence on a plane metal mirror) the integrating photodiode

still records a linear superposition of the two interferograms formed by each mode individually, as illustrated in Fig. 2.

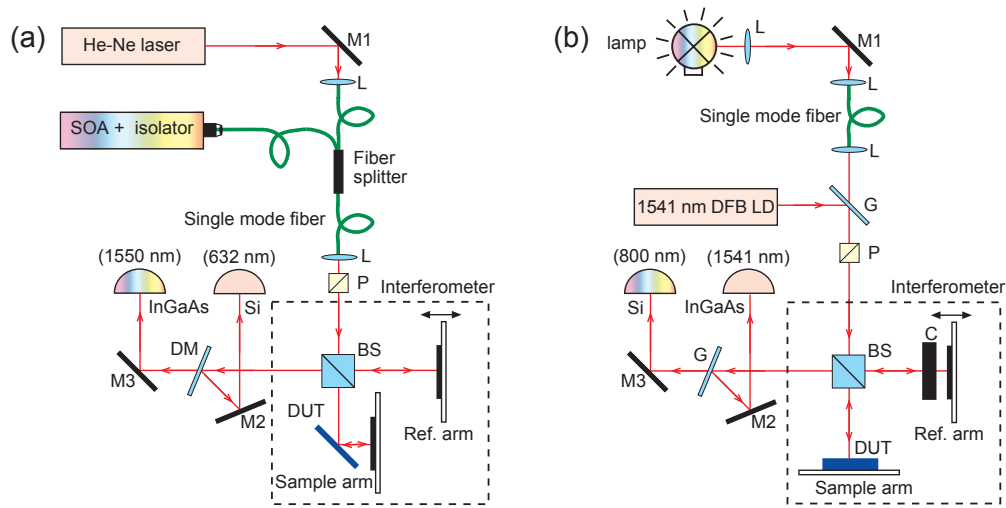


Fig. 1. Collinear fiber-coupled scanning white light interferometer for measurements of the spectrally resolved phase difference between polarization modes (a), and spatial fiber modes (b). SOA - centered at 1550 nm unseeded semiconductor optical amplifier (white light source), DFB LD - distributed feedback laser diode, He-Ne laser - Helium Neon laser (632 nm), M1, M2, M3 - silver mirrors, L - lenses, P - polarizer, BS - non-polarizing beam splitter, DM - dichroic mirror, G - thick glass plate, C - compensator. Collinear to the white light, the He-Ne (or DFB LD) beam is used to monitor the displacement of the reference mirror.

Processing the recorded linear superposition of the two interferograms (black curve in Fig. 2) with the Fourier Transform (which is a linear operation as well), we extract a complex response (i.e. the phase and amplitude) of the DUT. However, the separation of the phase and amplitude from the Fourier transform is not a linear operation. If the amplitude ratio between the modes varies rapidly with frequency, the retrieved Fourier phase exhibits arbitrary large artificial variations.

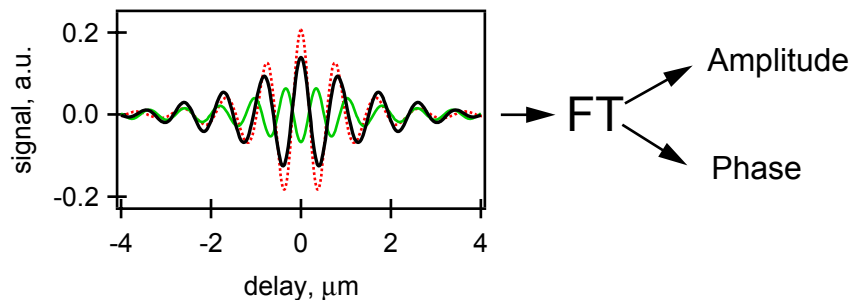


Fig. 2. Shows two interferograms (dotted red curve and solid green curve) of two individual modes, whose phases experience different phase retardations inside the interferometer. The phase and the complex amplitude are extracted from the Fourier transform of a linear superposition (black curve) of these two interferograms.

This situation can be illustrated with a vector diagram, shown in Fig. 3. For each mode, the green and the red vectors represent the complex response of the DUT at a certain optical

frequency. The measured response is the sum of both vectors, as shown with the black vector in Fig. 3. The situation with increasing optical frequency is illustrated by the animation in Fig. 3. In case the amplitude ratio between the modes does not change, the recorded phase spectrum is a linear superposition (weighted average) of the phase spectra of these two modes (see Fig. 3(a)). However if the amplitude ratio changes, the recorded phase is no longer the average. The degree of the amplitude-to-phase coupling depends on the phase difference between the modes: it is equal to zero when the phase shift between the modes is zero, and increases with growing phase difference (see Fig. 3(b), 3(c)). The strongest amplitude-to-phase coupling is observed when the phase difference is equal to π .

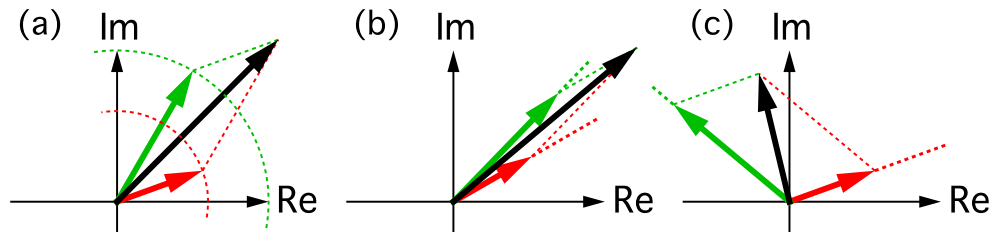


Fig. 3. (110 kB) Vector diagram for two individual modes (green and red vectors), and their sum (black vector). (a) The phase spectrum is the average when the amplitude ratio between the modes is constant. (b) The amplitude ratio between the modes changes, but the phase retardation for each mode is the same. (c) The phase for each mode is constant, but the amplitudes change with frequency. The sum exhibits strong phase oscillations.

These artificial oscillations in the Fourier phase are amplified by differentiation, which, for example, may clearly be observed in the GDD spectrum. Since these oscillations are caused by the dissimilar phase response of the DUT for each mode, the absolute phase difference between the modes can be obtained from a fit to the measured GDD data, as we demonstrate in the following sections on example of polarization and fiber modes.

3. Polarization modes

The absolute phase difference between the s- and p-polarizations of a dielectric multilayer DUT under 45° angle of incidence was measured with the setup shown in Fig. 1(a) and described in detail in [8]. The non-normal angle of incidence was chosen to generate a polarization dependent reflection in the DUT. A broadband polarizer was inserted before the input port of the interferometer to control the polarization.

We recorded three separate interferograms (one with s-polarized light, one with p-polarized light, and one with unpolarized input light with respect to the DUT), taken under identical measurement conditions. From the phase of the FT of each interferogram we calculated the GDD values (D_2). Figure 4 shows the spectrum (amplitude of the FT) and the GDD values (D_2) measured with p-, s- and unpolarized light. For p- polarized light the measured GDD values are nearly zero. The measured GDD for s-polarization has some variation, and also a different amplitude spectrum due to the fact that the complex reflectivity of the DUT is different for s- and p-polarizations.

With no phase difference between the modes the GDD measured with unpolarized light would be the average of the GDD values obtained with s- and p- polarizations. However, we observe very strong ($5'000 \text{ fs}^2$ peak-to-peak) artificial oscillations in the GDD spectrum for unpolarized light (see Fig. 4(a)). As it was explained in the previous section, the origin of these modulations is the different phase retardation accumulated by each mode inside the interferometer.

We are able to simulate the GDD oscillations experimentally observed with unpolarized light. For that we only use the recorded interferograms for s- and p- polarizations and assume

a linear phase difference between these polarization modes. The phase retardations inside the DUT for s- and p- polarization are

$$\varphi_s(\omega) = \iint D_{2,s}(\omega) d\omega^2 + C_{1,s}\omega + C_{0,s} \quad (1)$$

$$\varphi_p(\omega) = \iint D_{2,p}(\omega) d\omega^2 + C_{1,p}\omega + C_{0,p} \quad (2)$$

respectively, where $C_{1,s}$, $C_{0,s}$, $C_{1,p}$ and $C_{0,p}$ are the integration constants (experimentally not determined), $D_{2,s}$ and $D_{2,p}$ are the measured GDD values for s- and p- polarization. Since we are interested in the absolute phase difference between the modes, the undetermined linear phase term for one polarization (for example, p-) can be set to zero without any loss of generality. As a first step, we assumed a constant phase ($\Delta\varphi$) for the other (s-) polarization. From the linear sum of s- and p- interferograms we calculate the GDD values, as would be obtained with the unpolarized light (see solid black curve in Fig. 4(a)).

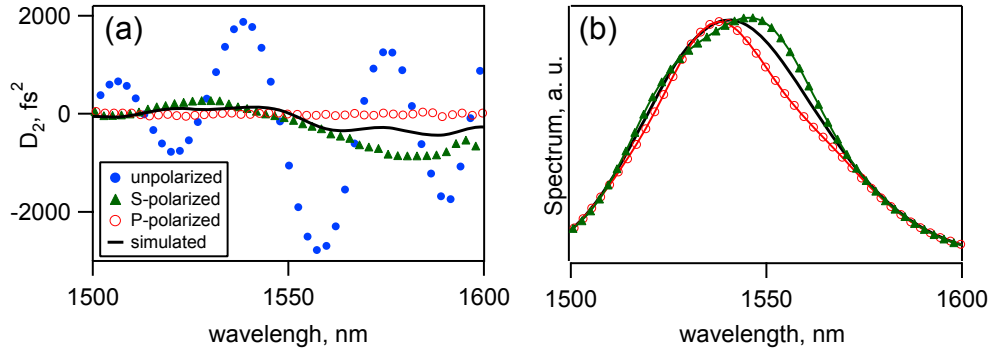


Fig. 4. (301 kB) (a) Measured GDD (D_2) for s-, p- and unpolarized light. (b) Spectral amplitude of the s- and p- polarized light. Solid black curves are the simulated GDD (a), and amplitude spectrum (b) when the phase difference between the modes increases.

As it can be seen from the animation in Fig. 4, the spectral position of these GDD oscillations depends on the first derivative of the amplitude ratio between the modes and the height of the peaks is related to the phase difference ($\Delta\varphi$). In general, $\Delta\varphi$ is a linear phase and therefore can be written as

$$\Delta\varphi = C_1\omega + C_0 \quad (3)$$

where C_1 and C_0 are free constants that are chosen as the fitting parameters to the GDD values measured with unpolarized light (see Fig. 5(a)).

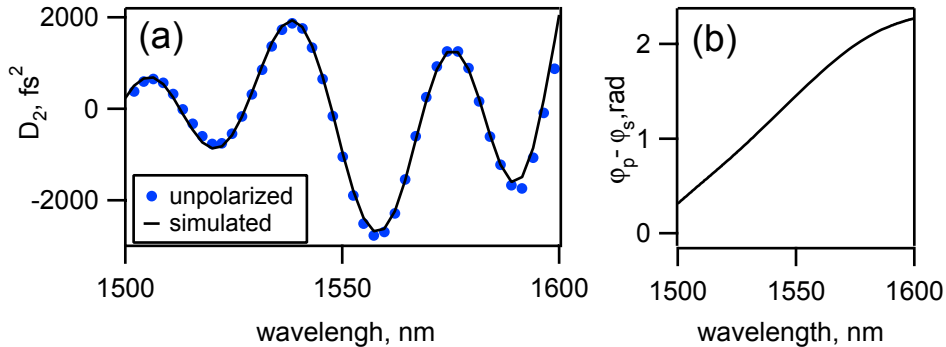


Fig. 5. (a) Measured GDD values (D_2) for the unpolarized light and the fit to the measurement. (b) The retrieved spectrally-resolved absolute phase difference between s- and p- polarizations.

The absolute phase difference between the polarization modes (see Fig. 5(b)) is then determined according to Eq. (1)-(3) from the GDD data measured with s-, p- and unpolarized light and the two fitting parameters, C_1 and C_0 .

4. Spatial modes

There is no easy way to separate collinear spatial modes, or create interference between them. The advantage of the technique presented in this paper is that no interference is needed to extract the absolute phase difference. As we had already discussed above, the recorded Fourier phase varies from the average phase only when the amplitude ratio between the modes changes. That allows for the absolute phase measurement between the fundamental and the higher order spatial fiber modes.

For this study we used a birefringent DUT inserted into a compensated scanning Michelson interferometer, as shown in Fig. 1(b). The source of a white light around 800 nm was an ordinary incandescent lamp. The white light was coupled into a fiber, and brought into the interferometer collinear with a reference beam from a distributed feedback laser diode (1541 nm).

As it was expected, a smooth optical spectrum and nearly zero GDD of the DUT have been observed (see dashed blue curve in Fig. 6(a)) when the light was coupled into a conventional fiber with single mode operation over the entire spectrum of measurement (THORLABS P1-3224-FC-2, cutoff < 620 nm). However, coupling the light into another single-mode fiber (THORLABS P1-5624-FC-2, cutoff < 950 nm), which has a transition from the single-mode to multi-mode regime within the region of measurement (see solid red curve in Fig. 6(a)), we observed rather strong artificial oscillations in the GDD spectrum. The spectral position of these oscillations corresponds to the single-to-multi-mode transition region of the fiber. Bending the fiber, we shift the transition region towards shorter wavelengths, and as a consequence, shift the spectral position (and apparently change the shape) of the GDD oscillations (see dotted green curve in Fig. 6(a)). Recall that the fiber is placed outside the interferometer only to create a superposition of two spatial modes. Any relative phase shift between the two modes occurring *outside* the interferometer does not affect the measured beat signal. The beat signal is present only due to the difference in phase and group delays for each spatial mode in the birefringent DUT placed *inside* the interferometer.

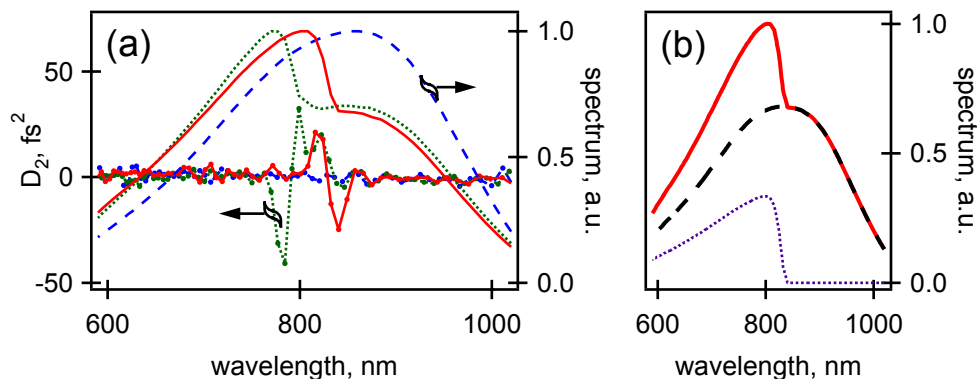


Fig. 6. (a) Measured GDD (D_2) and the spectrum for the P1-3224-FC-2 (dashed blue curves), for the unbent P1-5624-FC-2 (solid red curves), and the bended P1-5624-FC-2 (dotted green curves). (b) Simulated spectrum for the unbent P1-5624-FC-2 fiber (solid red curve), and the corresponding spectrums of the fundamental (dashed black curve) and higher excited mode (dotted violet curve).

To extract the phase difference between the fundamental and the higher excited modes of unbent P1-5624-FC-2 fiber, we first simulate the measured spectrum numerically. Outside the transition region i.e. below 800 nm and above 850 nm, the simulated data points are equal to the measured one. The transition region of the bended fiber is fitted with a polynomial multiplied with an error step-function, whose fit coefficient is the ratio (R) between the amplitudes of the fundamental and higher excited modes. Solid red curve in Fig. 6(b) shows the simulated unbent mode of the P1-5624-FC-2 fiber. From this simulated spectrum we then calculate the spectrum of the fundamental mode (dashed black curve in Fig 6(b)) under the assumption, that in multi-mode part of the original spectrum there are only two modes with the constant amplitude ratio R . This assumption is supported by the lack of artificial GDD oscillation in this regime and by the shape of the amplitude spectrum. Subtracting the fundamental mode (dashed black curve in Fig. 6(b)) from the simulated spectrum of the full mode (solid red curve in Fig. 6(b)), we obtain a spectrum of the higher-excited mode (dotted violet curve in Fig. 6(b)). For each of these modes we calculate an interferogram, and from the sum of these two interferograms we evaluate the GDD.

If the phase difference between the fundamental and higher excited mode would be zero, the corresponding GDD would also be zero. However, the measurement shows opposite (see Fig. 6(a)). Fitting a constant phase difference $\Delta\varphi$ between the modes, see Eq. (3), we reproduce the oscillations in the measured GDD data (see Fig. 7(a)). The amplitude of these oscillations strongly depends on the fitted phase, and the spectral position corresponds to the single-to-multi-mode transition region. Performing the same operation with the slightly bent P1-5624-FC-2 fiber, we also reconstruct the spectral shape of the recorded oscillations in GDD spectra (see Fig. 7(b)).

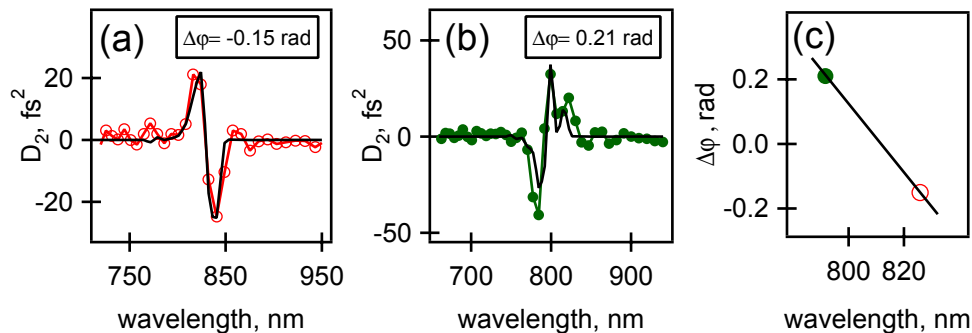


Fig. 7. (a) Measured (red curve, open circles) and simulated (solid black curve) GDD (D_2) for the unbent P1-5624-FC-2 fiber when the phase difference between the fundamental and higher excited mode is equal to (-0.15 rad). (b) Measured (green curve, filled circles) and simulated (solid black curve) GDD (D_2) for the slightly bended P1-5624-FC-2 fiber when the phase difference between the modes is equal to (0.21 rad). (c) Spectrally-resolved absolute phase difference between the fundamental and higher excited modes.

We can only obtain phase data from a rather narrow transition region (≈ 40 nm, ≈ 6 data points), which results in a single data point in Fig. 7(c). For this first-proof-of-principle demonstration we evaluated two measurements with the unbent (Fig. 7(a) and Fig. 7(c)) and slightly bended P1-5624-FC-2 fiber (Fig. 7(b) and Fig. 7(c)). Several measurements with differently bended fiber are necessary to obtain a full $\Delta\varphi(\omega)$ spectrum.

5. Conclusions

A novel method based on white-light interferometry and Fourier transform analysis has been demonstrated to measure the spectrally-resolved phase difference between orthogonal optical modes. Proof-of-principle measurements were performed with polarization and spatial fiber

modes. The precision of the retrieved phase difference depends critically on the spectral resolution and the GDD accuracy [8] of the corresponding measurements.

In addition, the presented discussion of the GDD data clearly demonstrates why strict polarization and modal control of the input beam is required for dispersion characterization with spectrally integrated white light interferometers.

We believe that our method can successfully be applied to a variety of other applications, for example the measurements of spectrally resolved modal dispersion of birefringent materials.

Acknowledgements

We would like to thank Prof. G. Guekos for providing the semiconductor optical amplifier as a white-light source. This work was supported by the Swiss National Science Foundation (NCCR).